

Room-Temperature Reaction between Laser Chemical Vapor Deposited Selenium and Some Metals

Akihiko Ouchi,[†] Zdeněk Bastl,[‡] Jaroslav Boháček,[§] Hideo Orita,[†] Koji Miyazaki,^{||} Setsuo Miyashita,^{||} Petr Bezdička,[§] and Josef Pola^{*-1}

National Institute of Advanced Industrial Science and Technology, AIST, Tsukuba, Ibaraki 305-8565, Japan, J. Heyrovský Institute of Physical Chemistry, 18223 Prague, Czech Republic, Institute of Inorganic Chemistry, Academy of Sciences of the Czech Republic, 25068 Řež, Czech Republic, Industrial Technology Center of Fukui Prefecture, Fukui 910-0102, Japan, and Laser Chemistry Group, Institute of Chemical Process Fundamentals, 16502 Prague, Czech Republic

Received November 4, 2003. Revised Manuscript Received June 30, 2004

Laser-chemical vapor deposition (LCVD) of elemental selenium onto the surface of several metals (Ag, Cu, Cd, Zn, Mg, Sn) has been achieved using photolytic decomposition of diethyl selenium, and the interaction between the deposited selenium coatings and the metal surface has been examined by X-ray photoelectron spectroscopy, Raman spectroscopy, X-ray diffraction, and electron microscopy. It is revealed that thin coatings of Se take part in a solid-state chemical reaction with Ag, Cd, Cu, Mg, and Zn substrates and demonstrated for the first time that the reaction between amorphous selenium and these metals (and not only Cu) does not require high temperatures but takes place at room temperature. The results reveal the feasibility of room-temperature selenization of metals.

Introduction

The synthesis of bulk, thin films and nanostructures of metal selenides is of continuing interest due to the many applications and potential uses of these species. Bulk and nanostructured compounds are well prepared in the liquid phase (e.g., refs 1–3), by high-temperature solid-state reactions,^{4–6} or at room temperature by high-energy ball-milling.⁷ Thin films of metal selenides have been prepared by many techniques such as sol–gel synthesis,⁸ chemical bath deposition (e.g., refs 9 and 10),

photochemically assisted bath deposition (e.g., ref 11), laser ablation,¹² vapor phase (e.g., refs 13 and 14), atomic layer,¹⁵ migration-enhanced (e.g., ref 16), molecular beam,¹⁷ and chemo (e.g., ref 18) epitaxy, metalloorganic chemical vapor (e.g., refs 19 and 20) and plasma-assisted (e.g., ref 21) deposition.

The simplest way to synthesize thin films of metal selenides is believed to be a direct reaction between the elemental metal and selenium at very high temperatures (several hundred °C) that favor formation of the crystalline compounds. However, it was demonstrated by electron microscopic studies that the solid–solid–

* Author to whom correspondence should be addressed. E-mail: pola@icpf.cas.cz.

[†] National Institute of Advanced Industrial Science and Technology.

[‡] J. Heyrovský Institute of Physical Chemistry.

[§] Institute of Inorganic Chemistry, Academy of Sciences of the Czech Republic.

^{||} Industrial Technology Center of Fukui Prefecture.

¹ Institute of Chemical Process Fundamentals.

(1) Steigerwald, M. L.; Alivisatos, A. P.; Gibson, J. M.; Harris, T. D.; Kortan, R.; Muller, A. J.; Thayer, A. M.; Duncan, T. M.; Douglass, D. C.; Brus, L. E. *J. Am. Chem. Soc.* **1988**, *110*, 3046.

(2) (a) Wang, W.; Geng, Y.; Yan, P.; Lin, F.; Xie, Y.; Qian, Y. *J. Am. Chem. Soc.* **1999**, *121*, 4062. (b) Henshaw, G.; Parkin, I. P.; Shaw, G. *Chem. Commun.* **1996**, 1095. (c) Liu, Y.; Cao, J.; Li, C.; Zeng, J.; Tang, K.; Qian, Y.; Zhang, W. *J. Cryst. Growth* **2004**, *261*, 508.

(3) Cumberland, S. L.; Hanif, K. M.; Javier, A.; Khitrov, G. A.; Strouse, G. F.; Woessner, S. M.; Yun, C. S. *Chem. Mater.* **2002**, *14*, 1576.

(4) Coustal, R. *J. Chim. Phys.* **1958**, *38*, 277.

(5) Yi, H. C.; Moore, J. J. *J. Mater. Sci.* **1990**, *25*, 1159.

(6) Williams, D. J.; White, K. M.; VanDereer, D.; Wilkinson, A. P. *Inorg. Chem. Commun.* **2002**, *5*, 124.

(7) Ohtani, T.; Motoki, M.; Koh, K.; Ohshima, K. *Mater. Res. Bull.* **1995**, *30*, 1495.

(8) Ptatschek, V.; Schreder, B.; Herz, K.; Hilbert, U.; Ossau, W.; Schottner, G.; Rahauser, O.; Bischof, T.; Lermann, G.; Materny, A.; Kiefer, W.; Bacher, G.; Forchel, A.; Su, D.; Giersig, M.; Muller, G.; Spanhel, L. *J. Phys. Chem. B* **1997**, *101*, 8898.

(9) (a) Kainthla, R. C.; Pandya, D. K.; Chopra, K. L. *J. Electrochem. Soc.* **1980**, *127*, 277. (b) Chen, R.; Xu, D.; Guo, G.; Gui, L. *Electrochem. Commun.* **2003**, *5*, 579.

(10) Riveros, G.; Guillemoles, J. F.; Lincot, D.; Meier, H. G.; Froment, M.; Bernard, M. C.; Cortes, R. *Adv. Mater.* **2002**, *14*, 1286.

(11) (a) Kumaresan, R.; Ichimura, M.; Arai, E. *Thin Solid Films* **2002**, *414*, 25. (b) Zhao, W.-B.; Zhu, J.-J.; Chen, H.-Y. *J. Cryst. Growth* **2003**, *252*, 587.

(12) Perna, G.; Capozzi, V.; Plantamura, M. C.; Minafra, A.; Biagi, P. F.; Orlando, S.; Marotta, V.; Giardini, A. *Appl. Surf. Sci.* **2002**, *186*, 521.

(13) (a) Russak, M. A.; Reichman, J.; Witzke, H.; Deb, S. K.; Chen, S. N. *J. Electrochem. Soc.* **1980**, *127*, 725. (b) Hamdadou, N.; Bernède, J. C.; Khelil, A. *J. Cryst. Growth* **2002**, *241*, 313.

(14) Jeyakumar, R.; Lakshmi Kumar, S. T.; Rastogi, A. C. *Mater. Res. Bull.* **2002**, *37*, 617.

(15) (a) Akinaga, H.; Tanaka, K. *Appl. Surf. Sci.* **1994**, *82/83*, 298. (b) Guziewicz, E.; Godlewski, M.; Kopalko, K.; Lusakowska, E.; Dynowska, E.; Guziewicz, M.; Godleski, M. M.; Phillips, M. *Thin Solid Films* **2004**, *446*, 172.

(16) Gaines, J. M.; Petruzzello, J.; Greenberg, B. *J. Appl. Phys.* **1993**, *73*, 2835.

(17) Feng, P. X.; Riley, J. D.; Leckey, R. C. G.; Ley, C. *J. Phys. D, Appl. Phys.* **2001**, *34*, 1293.

(18) Ignatenko, P. I. *Izv. Akad. Nauk SSSR, Neorg. Mat.* **1989**, *25*, 563; *Chem. Abstr.* 111/15541.

(19) Sritharan, S.; Jones, K. A.; Motyl, K. M. *J. Cryst. Growth* **1984**, *68*, 656.

(20) Prete, P.; Lovergine, N.; Tapfer, L.; Zanotti-Fregonara, C.; Mancini, A. M. *J. Cryst. Growth* **2000**, *214/215*, 119.

(21) Lakshmi Kumar, S. T.; Rastogi, A. C. *J. Appl. Phys.* **1994**, *76*, 3068.

state reaction between Cu and Se yielding crystalline Cu_xSe_y compounds occurs^{22–26} at room temperature and that a similar selenization reaction between solid Se and Ag takes place^{27,28} at as low as 60 °C. In those studies, Se has been brought into contact with the metal surface through its evaporation and deposition, and the resulting growth of crystalline metal selenides was considered as due to the atoms' diffusion.

We have previously reported on UV laser-induced gas-phase photolysis of several organoselenium compounds for chemical vapor deposition of selenium films.^{29–33} Dialkyl selenides^{29,30,32} and selenophene^{31,33} irradiated by ArF or KrF lasers were efficiently photolyzed into selenium, which produced thin Se layers upon deposition to Al and glass. Here we report that the UV laser photolysis of gaseous diethyl selenium and consecutive Se deposition onto several metals results in some cases (Ag, Cu, Cd, Mg, Zn) in the formation of metal selenide. These findings provide extension to the earlier published room-temperature solid–solid-state reaction between selenium and copper and reveal that the solid–solid-state room-temperature reaction between selenium and metals is a more common process.

Experimental Section

Chemical vapor deposition of selenium was achieved by laser photolysis of gaseous diethyl selenium in a reactor described previously.³² Briefly, the reactor consisted of two orthogonally positioned Pyrex tubes (both 3 cm in diameter), one (9 cm long) fitted with two quartz windows and the other (13 cm long) furnished with two KBr windows. It was equipped with a sleeve with rubber septum and PTFE valve connecting it to a standard vacuum line and accommodated metal sheets (area of $\sim 1 \text{ cm}^2$ or less) that were loosely positioned on its bottom. The laser photolysis of diethyl selenium (20 Torr) in nitrogen (total pressure 760 Torr) was conducted using an LPX 210i laser (ArF) operating at 193 nm with a repetition frequency of 10 Hz and delivering fluence of 55 mJ/cm^2 (measured by a Gentec ED-500 joulemeter connected to a Gold Classic 9500 storage oscilloscope) within an effective area of 5 cm^2 . One and three subsequent photolytic runs (each with 6000 pulses to achieve $\sim 70\%$ depletion of diethyl selenium) were accomplished to deposit selenium films of different thickness. The photolytic progress was checked by infrared spectroscopy (a Shimadzu FTIR 4000 spec-

trometer) at 1198 cm^{-1} . The used irradiating conditions made possible efficient decomposition of diethyl selenium to elemental selenium without blocking the entrance window with selenium particles. After the photolysis and the deposition of selenium films, the reactor was evacuated and the metal sheets were transferred for the measurement of their surface properties using different physical methods.

The XPS measurements were carried out using a Gammadata Scienta ESCA 310 electron spectrometer equipped with a high-intensity monochromatized Al $K\alpha$ X-ray source and a 60-cm-diameter hemispherical analyzer with multichannel detector. The power on the X-ray source was kept constant at 3 kW. The energy resolution determined from the slope of the Fermi edge of silver was 0.4 eV. Some measurements were also performed using a VG ESCA 3 MkII spectrometer with unmonochromatized Mg $K\alpha$ radiation. Both spectrometers were calibrated to the Au $4f_{7/2}$ peak at 84.00 eV. The pressure in the analyzer chamber during spectra acquisition was in the 10^{-9} mbar range. The spectra of Se 3d, C 1s, O 1s, Ag 3d, Cu 2p, Cd 3d, Mg 2s, Sn 3d, and Zn 2p photoelectrons were measured. No static charging during spectra measurement was observed.

The measurements of Raman spectra were carried out at room temperature with a LabRam Infinity spectrometer (Jobin Yvon). The spectrometer was equipped with a He–Ne laser (632.8 nm, 15 mW), a microscope sample stage, and a CCD detector. The resolution of the spectrometer was less than 5 cm^{-1} .

Field emission scanning electron microscopy (SEM) measurements were performed on a dual-stage DS-720 Topcon electron microscope (accelerating voltage 5 kV).

X-ray diffraction measurements were carried out with a Rigaku RAD-RVC instrument (Cu $K\alpha$ radiation, 40 kV, 150 mA), and qualitative analysis was performed with the DiffractPlus software package³⁴ or Bede ZDS program package³⁵ and JCPDS PDF-2 database.³⁶

TEM analysis (particle size and phase analysis) was conducted on a Philips 201 transmission electron microscope at 80 kV on deposited materials scraped from the metal substrates and transferred to a Formvar 1595 E (Merck) membrane-coated Cu grid. Process diffraction³⁷ was used to evaluate and compare measured electron diffraction patterns with an XRD diffraction database.³⁵

Diethyl selenium (purity better than 98%) was prepared using the reported procedure³⁸ and distilled prior to use. The sheets of silver, copper, cadmium, zinc, magnesium, and tin (purity better than 99.99%) were purchased from Soekawa Chemicals and mechanically cleared from their passivating oxide layer that was scraped off under nitrogen atmosphere.

Results and Discussion

The ArF laser irradiation of the gaseous diethyl selenium in nitrogen atmosphere results in efficient cleav-

(22) Morikawa, H. *Jpn. J. Appl. Phys.* **1970**, *9*, 607.

(23) Kaito, C. *J. Cryst. Growth* **1974**, *24/25*, 563.

(24) Shiojiri, M.; Kaito, C.; Saito, Y.; Teranishi, K.; Sekimoto, S. *J. Cryst. Growth* **1981**, *52*, 883.

(25) Nagashima, S.; Fukuchi, E.; Ogura, I. *Appl. Surf. Sci.* **1991**, *48/49*, 44.

(26) Kaito, C.; Nonaka, A.; Kimura, S.; Suzuki, N.; Saito, Y.; *J. Cryst. Growth* **1998**, *186*, 386.

(27) Safran, G.; Kensch, P.; Gunter, V. R.; Barna, P. B. *Thin Solid Films* **1992**, *215*, 147.

(28) Safran, G.; Geszti, O.; Radnoczi, G.; Barna, P. B. *J. Cryst. Growth* **1998**, *317*, 72.

(29) Pola, J.; Bastl, Z.; Šubrt, J.; Ouchi, A. *Appl. Organomet. Chem.* **2001**, *15*, 924.

(30) Pola, J.; Bastl, Z.; Šubrt, J.; Ouchi, A. *Appl. Surf. Sci.* **2001**, *172*, 220.

(31) Pola, J.; Bastl, Z.; Šubrt, J.; Ouchi, A. *Appl. Organomet. Chem.* **2000**, *14*, 715.

(32) Pola, J.; Vitek, J.; Bastl, Z.; x3Ubrt, J. *J. Organomet. Chem.* **2001**, *640*, 170.

(33) Pola, J.; Ouchi, A. *J. Org. Chem.* **2000**, *65*, 2759.

(34) *DiffractPlus*, version 8.0; Bruker AXS, 2002.

(35) *Bede ZDS*, version 4.0. Bede Inc., 2000.

(36) *JCPDS PDF-2 database*, International Centre for Diffraction Data: Newtown Square, PA, release 52, 2002.

(37) Lábár, J. L. In *Proceedings of EUREM12*; Frank, L., Ciampor, F., Eds.; Czechoslovak Society for Electron Microscopy: Brno, 2000; p 1379.

(38) Bird, Y. M. L.; Chalenger, F. *J. Chem. Soc.* **1942**, 570.

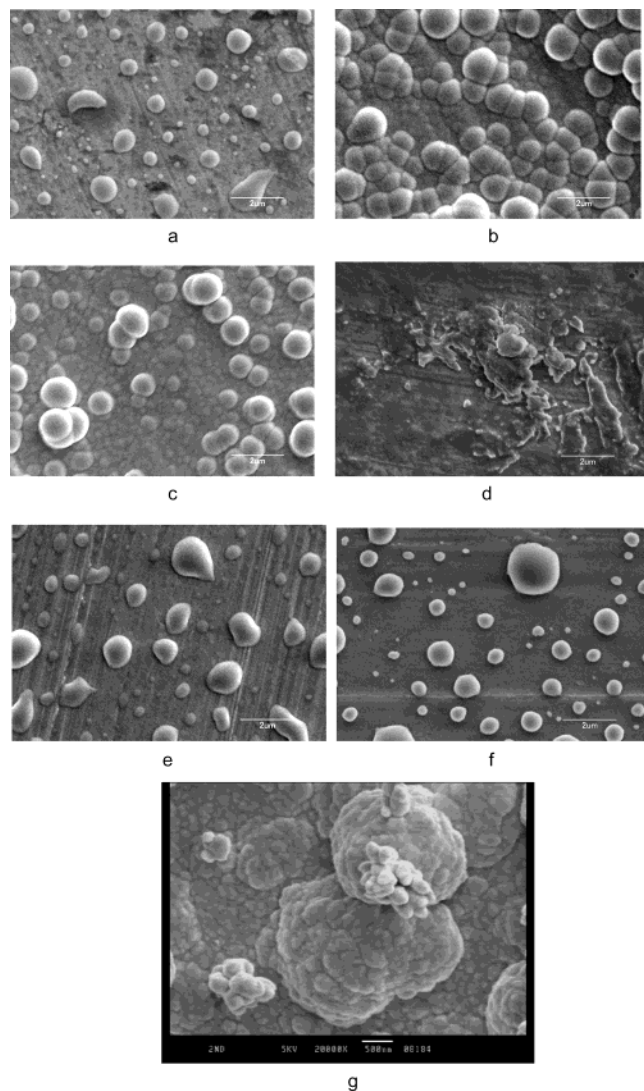


Figure 1. SEM images of selenium deposited onto sheets of Sn (a), Ag (b, g), Cu (c), Cd (d), Zn (e), and Mg (f). (Bar is 2 (a–f) and 0.5 μm (g).)

age of both C–Se bonds, formation of C_1 – C_4 hydrocarbons, and instant formation of a white selenium fog that slowly descends onto the reactor glass walls where it creates initially white and later pinkish coatings of amorphous selenium.²⁹ This photolysis affording ethene as a major product takes place mostly as β -elimination of ethene (a major path: $(\text{C}_2\text{H}_5)_2\text{Se} \rightarrow \text{Se} + 2\text{C}_2\text{H}_4 + \text{H}_2$) and is accompanied by minor radical routes giving rise to propane, propene, methane, and ethyne.²⁹ All the hydrocarbons are inert and do not interfere with the deposition of elemental selenium.

The selenium coatings deposited on quartz, glass, and KBr stay whitish for an extended period of time. Their whitish color allows one to discern among possible Se allotropes (amorphous selenium (a-Se) and crystalline trigonal, α - and β -monoclinic Se) and indicates an a-Se phase. The selenium coatings deposited on metals do not stay white and change the metal's appearance. Those on tin and magnesium become transparent and lend the initially shiny metal surface a darker dull appearance. The shiny silver and copper sheets get instantly (within 30 s after the photolysis) deep black; the cadmium and zinc plates respectively change their grayish color less rapidly (within 10–20 min after the

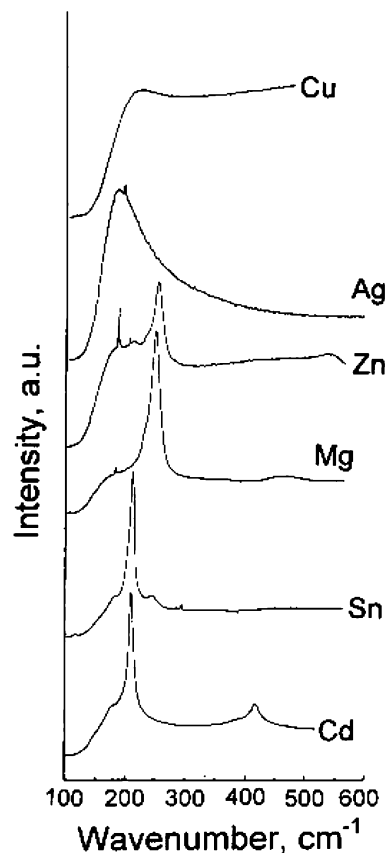


Figure 2. Raman spectra of Se coatings deposited on different metals. The curves have the maximum at 180 (Ag), 200 (Cu), 181 and 253 (Zn), 255 (Mg), 212 and 253 (Sn), 208 and 415 cm^{-1} (Cd).

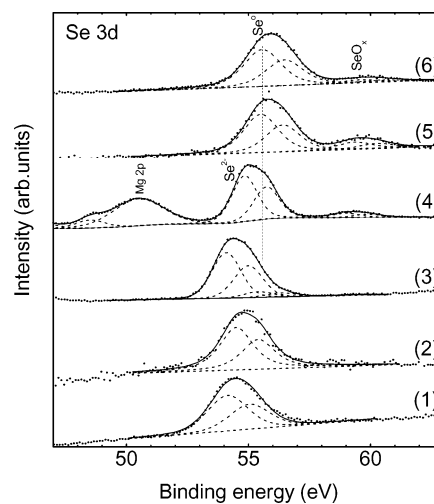


Figure 3. Fitted spectra of Se 3d core level electrons taken from Se deposited on (1) Ag, (2) Cu, (3) Cd, (4) Mg, (5) Sn, and (6) Zn.

photolysis) into brown and yellowish shade. These color changes indicate either chemical reaction between selenium and metal or they can be ascribed to a change of amorphous to crystalline Se phase.

Electron Microscopy. The SEM images of the photodeposited coatings on Ag, Cu, Cd, Zn, Mg, and Sn are given in Figure 1. It is revealed that morphology patterns of Se are represented by typical ball-like morphology of amorphous selenium.³⁹ The size of islands ranges within ~ 0.1 – $1 \mu\text{m}$. The growth of selenium thin

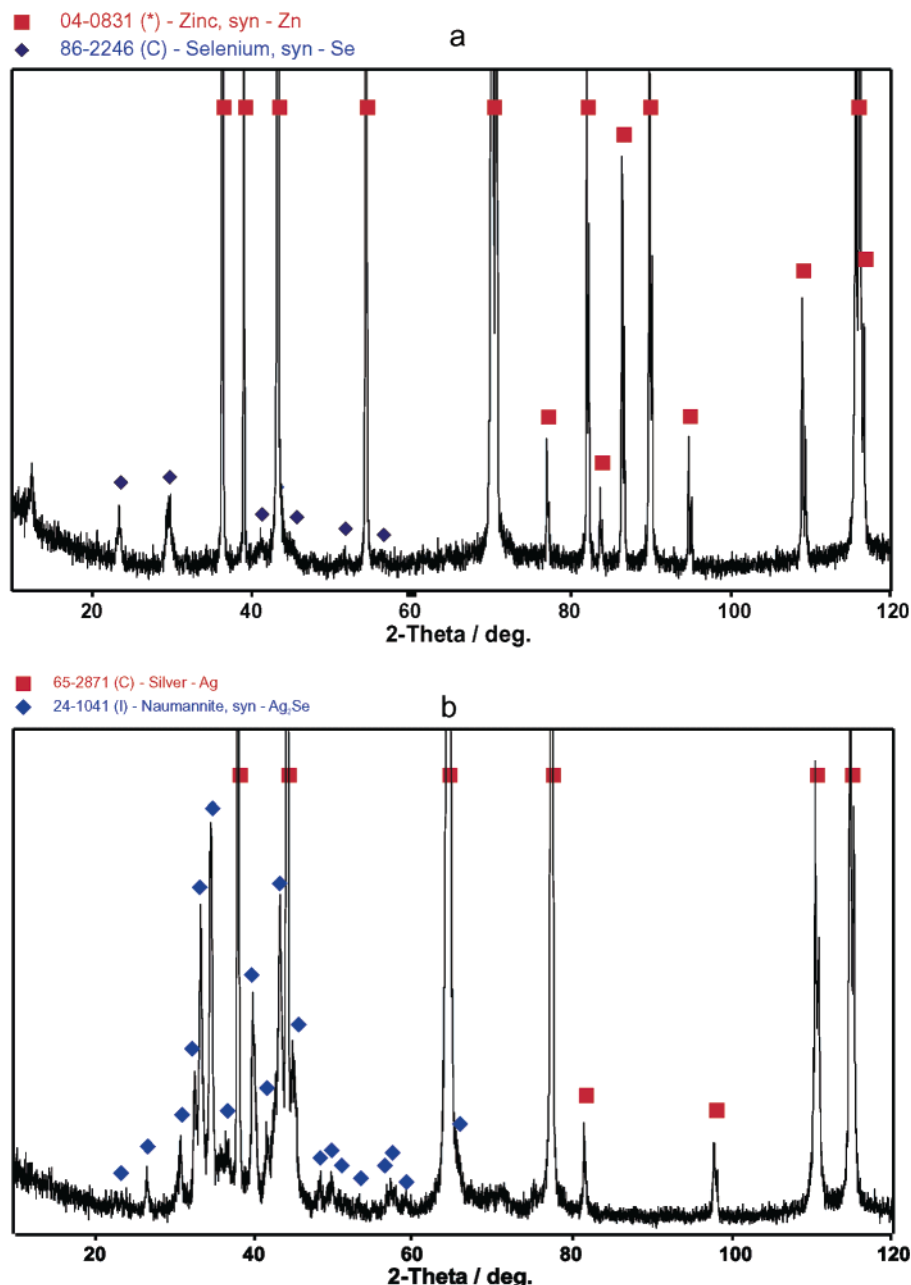


Figure 4. Powder XRD pattern of Se deposited on Zn (a) and Ag (b).

films at low temperatures on different substrates was explained³⁹ as taking place through motion of Se atoms on the surface and their incorporation into islands. We presume that the laser photolysis results in the gas-phase formation of nanosized Se bodies that deposit onto the metal surface and can increase their size via coalescence with later deposited particles. The SEM image then reflects the presence of large round-shaped bodies sitting on a layer formed from particles smaller than 0.1 μm .

The large bodies do not have the typical smooth surface of a-Se but rather possess a rough surface that is indicative of crystallization. This feature is best seen at larger magnification (Figure 1g).

Raman Spectra. The Raman spectra of the coatings produced by the chemical vapor deposition (CVD) of

selenium onto the metals are shown in Figure 2. It is seen that those of the coatings on zinc, cadmium, magnesium, and tin possess a narrow band centered, in the given order, at 253, 208, 255, and 212 cm^{-1} , whereas those of the coatings on Ag and Cu show a broad band respectively centered at ~ 180 and ~ 200 cm^{-1} . These features are to be discussed in terms of the well-known longitudinal optical (LO) mode in films of MgSe (252 cm^{-1} ⁴⁰), CdSe (210 cm^{-1} ⁴¹), CuSe₂ (260 cm^{-1} ⁴²), CuSe (263 cm^{-1} ⁴³), ZnSe (254 cm^{-1} ⁴⁴), Ag₂Se

(40) Kozielski, M.; Szybowicz, M.; Firszt, F.; Legowski, S.; Meczynska, H.; Szatkowski, J.; Paszkowicz, W. *Cryst. Res. Technol.* **1999**, *34*, 699.

(41) Feng, Z. C.; Becla, P.; Kim, L. S.; Perkovitz, S.; Feng, Y. P.; Poon, H. C.; Williams, K. P.; Pitt, G. D. *J. Cryst. Growth* **1994**, *138*, 239.

(42) Fritz, H. P.; Pöll, E. *Z. Naturforsch.* **1993**, *48b*, 697.

(43) Ishii, M.; Shibata, K.; Nozaki, H. *J. Solid State Chem.* **1993**, *105*, 504.

(39) Özenbas, M. *J. Mater. Sci.* **1987**, *22*, 1419.

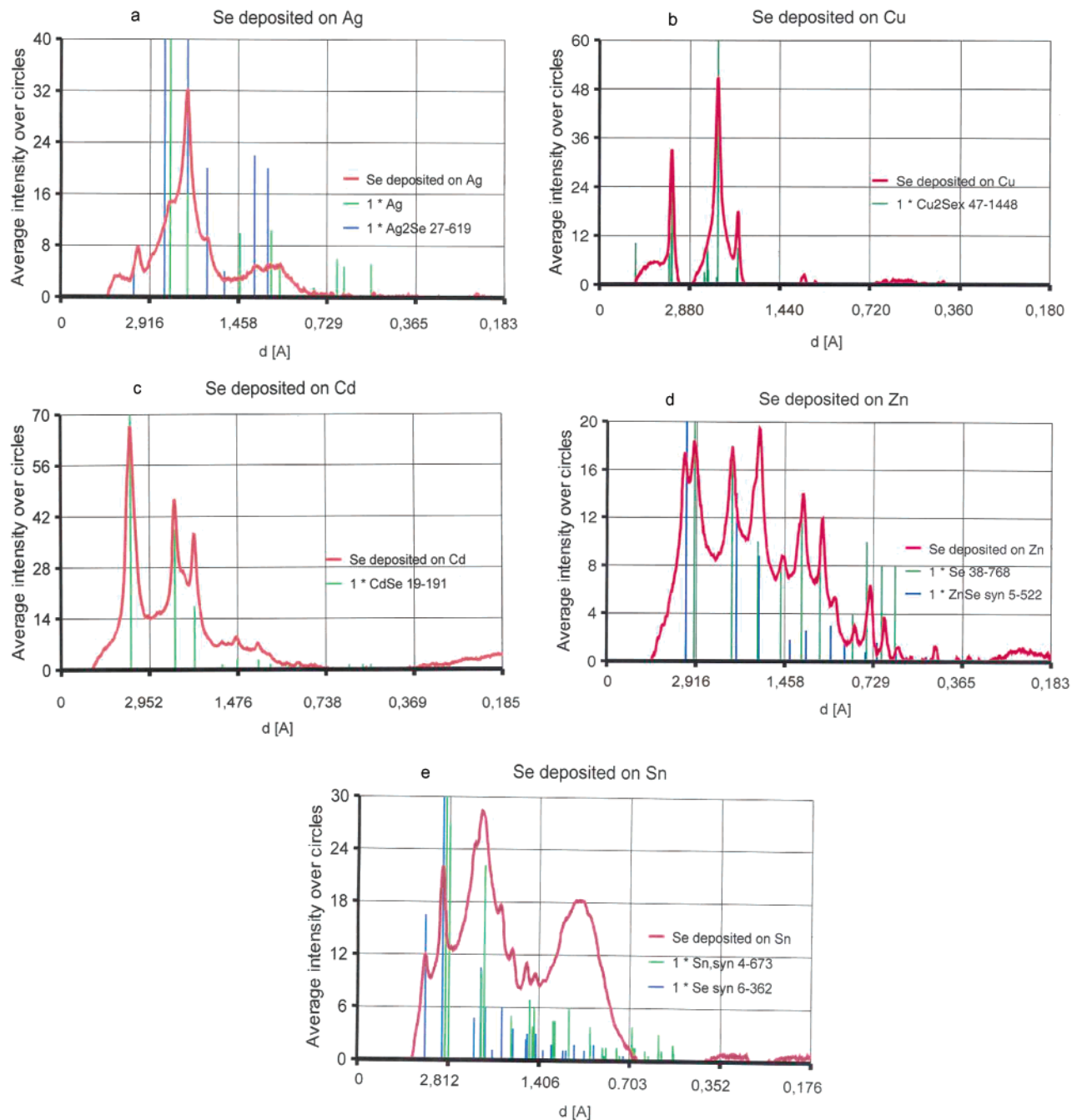


Figure 5. Diffraction pattern of the deposited Se on Ag (a), Cu (b), Cd (c), Zn (d), and Sn (e) as compared with that of the metal, selenide, and selenium (diffraction patterns from XRD diffraction database³⁵).

(100–200 cm^{-1} ⁴⁵), and SnSe_2 (135 cm^{-1} ⁴⁶) and of Raman spectrum of a-Se films that display a broad peak at ~ 250 cm^{-1} ^{47,48}, mainly due to disordered Se chains and a shoulder at ~ 235 cm^{-1} due⁴⁹ to trigonal Se (t-Se) existing in a-Se.

(44) Pages, O.; Ajjoun, M.; Laurenti, J. P.; Chauvet, C.; Tournie, E.; Faurie, J. P. *Appl. Phys. Lett.* **2000**, *77*, 519.

(45) Ishii, M.; Wada, H. *Mater. Res. Bull.* **1993**, *28*, 1269.

(46) Yang, A.-L.; Wu, H.-Z.; Li, Z.-F.; Qiu, D.-J.; Chang, Y.; Li, J.-F.; McCann, P. J.; Fang, X. M. *Chin. Phys. Lett.* **2000**, *17*, 606.

(47) Lucovsky, G.; Mooradian, A.; Taylor, W.; Wright, G. B.; Keezer, R. C. *Solid State Commun.* **1967**, *5*, 113.

(48) Lucovsky, G. In *The Physics of Selenium and Tellurium*, Proc. Int. Conf. Königstein, Germany; Gerlach, E., Grosse, P., Eds.; Springer-Verlag: Berlin, 1979; p 178.

(49) Yashiro, M.; Nishina, Y. In *The Physics of Selenium and Tellurium*, Proc. Int. Conf., Königstein, Germany; Gerlach, E., Grosse, P., Eds.; Springer-Verlag: Berlin, 1979; p 206.

The Raman spectral patterns of the coatings on Cu and Ag do not correspond either to amorphous or trigonal selenium and rather can be assigned to the metal selenides, despite the fact that the peaks' maximums do not precisely match the literature values. Similarly, the Raman spectrum of the coating on Cd reveals the presence of CdSe but not that of Se. Apart from the LO peak at 208 cm^{-1} , the 2LO peak at 415 cm^{-1} is also apparent. The Raman spectra of the coatings on Zn and Mg show a band at 250 cm^{-1} , which assigns to both a-Se and the metal selenides and does not allow discernment between these entities. The band at 250 cm^{-1} has a shoulder at ~ 235 cm^{-1} , which corresponds to t-Se phase. The Raman band of the coating on Sn relates neither to Se nor to SnSe_2 and may be associated with a yet unreported selenide form.

We note that the presence of a band at 235 cm^{-1} in the spectra indicates the crystallization of α -Se. This is in keeping with the SEM pattern (Figure 1g). We admit that some crystallization could occur during the collection of the Raman spectra (laser heating), since it is known that amorphous selenium has a low crystallization temperature ($<150\text{ }^\circ\text{C}$).

X-ray Photoelectron Spectra (XPS). The XPS analysis of the deposited selenium on the metals reveals^{50,51} the presence of elemental selenium and metal selenides (Figure 3). The binding energy of the Se $3d_{5/2}$ core level electrons of elemental selenium amounts to $\sim 55.3\text{ eV}$. The spectra of the Se deposited on Ag, Cu, Cd, and Mg substrates show also a contribution of a subband (in the given order at 54.2, 54.5, 54.1, and 54.6 eV) that is consistent with values reported in the literature⁵⁰ for metal selenides. The small contribution of selenium oxide (at 59.5 eV) observed in the spectra of Mg, Sn, and Zn samples is due to a minor oxidation of the film taking place during the transfer of the samples to the spectrometer.

X-ray Diffraction Analysis (XRD). XRD patterns of the Se coatings on the metal sheets do not provide good evidence of the nature of the interface layer (a layer between the metal surface and Se coating), since this layer is obviously rather thin. They reveal that the deposited amorphous selenium changes into crystalline selenium, which was observed on Cd, Sn, and Zn. The metal selenide was identified only on Ag. The pattern of XRD films on Cu and Mg reveals neither crystalline selenium nor selenide. The illustration of the crystalline selenium (Se on Zn) and metal selenide (Se on Ag) phases is given in Figure 4.

Electron Diffraction Analysis. The electron diffraction patterns of the selected coatings areas reveal the presence of crystalline selenium, and in the case of the coatings on Ag, Cu, Cd, and Zn, they show good fits to interlayer distances of metal selenides. We note that panels a–d of Figure 5 were chosen from among several electron diffraction patterns and represent examples wherein metal selenide is not accompanied with selenium.

We consider that a few tens of micrometers thick (initially Se) films provided enough material for electron diffraction analysis and that the corresponding TEM images of the coatings scraped from the metal surface (given for illustration in Figure 6) reflect crystalline phases of the selenides.

The above experimental findings thus reveal that the laser-induced gas-phase photolysis of diethyl selenium results in the formation of elemental selenium that deposits on quartz, glass, KBr, magnesium, and tin as whitish coatings that retain their color for an extended period of time. The whitish color of the Se coatings allowed discernment among possible Se allotropes (α -Se, and crystalline trigonal, α - and β -monoclinic Se) and indicated α -Se phase.

The selenium coatings deposited on silver, copper, cadmium, and zinc quickly change their initially white color into deep black (Ag and Cu), brown (Cd), and

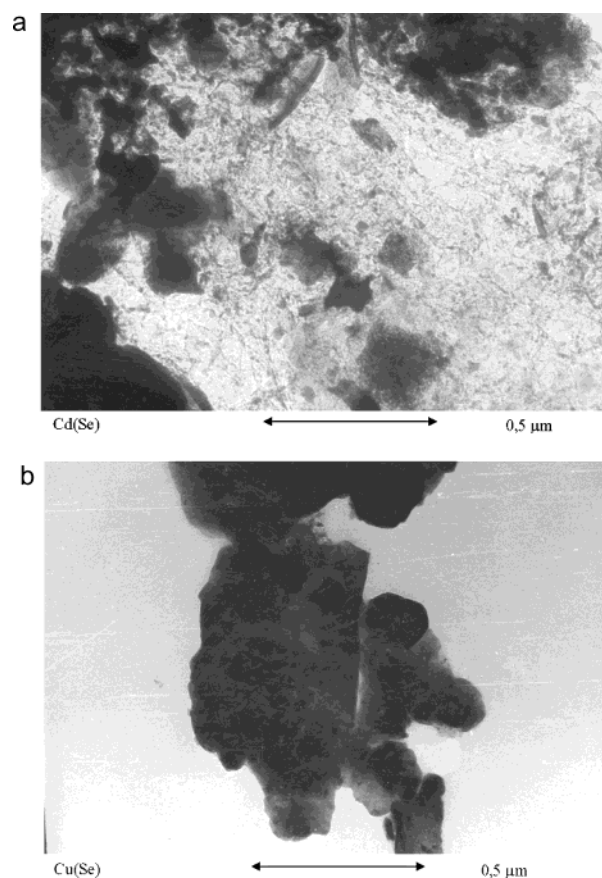


Figure 6. TEM images of the deposit on Cd (a) and on Cu (b).

Table 1. Different Forms of Se Observed by Different Analyses

metal	Raman spectrum	XRD analysis	electron diffraction	X-ray photoelectron spectrum	color
Ag	Se ²⁻	Ag ₂ Se	Ag ₂ Se, Se	Se ²⁻	black
Cu	Se ²⁻		Cu ₂ Se, Se	Se ²⁻	black
Cd	Se ²⁻	Se	CdSe, Se	Se ²⁻	brown
Mg	Se ²⁻ and/or α -Se t-Se			Se ²⁻	white
Zn	Se ²⁻ and/or α -Se t-Se	Se	ZnSe, Se	Se	yellow
Sn	Se ²⁻ (?)	Se	Se	Se	white

yellow (Zn). The scrutiny of the coatings by X-ray photoelectron, Raman spectra, electron microscopy, and X-ray diffraction analysis (Table 1) revealing that the selenium films change their initially amorphous phase into crystalline phase, react with the metal to yield metal selenides, or both.

The room-temperature reaction between selenium and metal was proved for Ag, Cu, Cd, Mg, and Zn and not for Sn. The different feasibility of the metal selenide formation with different metals is most likely due to different metal electropositivity and different metal/Se diffusion. The larger exothermic release takes place upon formation of metal selenides from more electropositive metals; heats of formation of metal selenides indicate^{52,53} that the easiest formation of metal selenides should take place with Mg and Zn. We believe, however, that the room-temperature formation of metal selenides

(50) NIST X-ray Photoelectron Spectroscopy Database, version 2.0; U.S. Department of Commerce: NIST, Gaithersburg, MD, 1997.

(51) Canava, B.; Vigneron, J.; Etcheberry, A.; Guilemoles, J. F.; Lincot, D. *Appl. Surf. Sci.* **2002**, *202*, 8.

(52) *Gmelin Handbuch der Anorganischen Chemie*; Springer-Verlag: Berlin, 1981; Vol. 3a (Selenium).

will be primarily controlled by diffusion, and we assume that mutual diffusion of both counterparts will be of high importance for the formation of a metal–selenium phase, wherein metal selenide compound will be produced (initially in amorphous and later in crystalline state) after the proper metal/Se ratio has been attained. Experimental data for diffusion of Se in metals and for diffusion of metals in selenium are missing, and the prediction of relative diffusion ability of different metals in Se and of Se in different metals is not possible in view of the known irregularities in diffusions of similar entities (e.g., anomalously high diffusion at low temperatures of Cd in CdS and of Cu and Ag in ZnS⁵⁴). Simple prediction of relative diffusion ability of different metals in Se and of Se in different metals is also hampered by recent observation that the relative extent of diffusion of Cu and Se is dependent on the Cu and Se particle size.²⁶

It is obvious that the deposited selenium can react with the metal only at the contact area and within their inner layers (due to diffusion of metal atoms into selenium and Se atoms into metal²⁶) and that this

reaction does not take place within outer layers of metal and selenium phases. It is thus plausible to assume that the detected crystalline Se phase occurs mostly in outer Se layers and in the round-shaped Se particles that change into crystalline spherulites. This feature is well illustrated for Se deposited on Ag (Figure 1g).

Conclusions

Our results reveal for the first time that the reaction between the metals and selenium does not require high temperatures (several hundred °C⁵⁵) and that it occurs at ambient temperature. The results could find very important applications in technologies that benefit from fabrication of metal chalcogenides at ambient temperatures (e.g., solar cell applications, synthesis of metal chalcogenide thin films or nanoclusters on the surface of or within a body of polymers).

Acknowledgment. The authors thank Ms. Tomoko Watanabe for the SEM measurements. This work was supported by the Ministry of Education, Youth and Sports of the Czech Republic (Grant ME 611).

CM035117B

(53) Mills, K. C. *Thermodynamic Data for Inorganic Sulfides, Selenides and Tellurides*; Butterworths: London, 1974.

(54) *Physics and Chemistry of II–VI Compounds*; Aven, M., Prener, J. S., Eds.; North Holland Publ. Co.: Amsterdam, 1967.

(55) Kwestro, W. In *Preparative Methods in Solid State Chemistry*; Hagenmuller, P., Ed.; Academic Press: New York, 1972; p 263 and refs therein.